

VISUAL SENSITIVITY TO SPATIALLY SAMPLED MODULATION IN HUMAN OBSERVERS

JEFFREY B. MULLIGAN* and DONALD I. A. MACLEOD

Department of Psychology, University of California at San Diego, Mail Code C-009,
La Jolla, CA 92093, U.S.A.

(Received 8 December 1986; in revised form 20 March 1990)

Abstract Thresholds were measured for detecting spatial luminance modulation in regular lattices of visually discrete dots. Thresholds for modulation of a lattice are generally higher than the corresponding threshold for modulation of a continuous field, and the size of the threshold elevation, which depends on the spacing of the lattice elements, can be as large as a one log unit. The largest threshold elevations are seen when the sample spacing is 12 min arc or greater. These results are similar to those observed by Burr, Ross and Morrone [*Vision Research*, 25, 717-727 (1985)], who proposed an explanation based on a compressive point nonlinearity. Although their explanation is not consistent with the present data, the results may be explained in terms of nonlinear saturation of a *spatially opponent* stage early in the visual pathway. Theories based on response compression cannot explain the further observation that the threshold elevations due to spatial sampling are also dependent on modulation frequency: the greatest elevations occur with higher modulation frequencies. The idea that this is due to masking of the modulation frequency by the spatial frequencies in the sampling lattice is considered.

Spatial modulation sensitivity Sampling Spatial masking

INTRODUCTION

It has been suggested that the early stages of the visual system act like a set of filters, each tuned to a particular band of spatial frequencies (Campbell & Robson, 1968), and a large body of evidence has accumulated supporting this view (for a review see Olzak & Thomas, 1986). Many of the studies supporting this view have employed sinusoidal luminance gratings as stimuli. The mathematical properties of gratings make them useful for investigating linear aspects of the visual system, but there are a number of easily observed visual phenomena which display clearly nonlinear properties. Filter-bank type models of the visual system, such as those of Wilson and Bergen (1979), have usually been designed to predict threshold data; they must be embellished in order to predict the appearance of suprathreshold aspects of objects, such as brightness or apparent contrast (Georgeson & Sullivan, 1975).

The Craik Cornsweet illusion (Cornsweet, 1970, p. 273) is an example of how a small, local feature (a high-pass filtered edge) can exert an

effect on the subjective brightness of distant areas although there are no low-frequency Fourier components in the pattern. Land's retinex model of color appearance (Land & McCann, 1971) similarly stresses the importance of sharp edges and allows them to act over arbitrarily large distances. Sharp edges also seem to play an important role in the "filling in" of retinally stabilized images.

In our earlier work, we reported how the density of texture elements could produce illusory changes in the brightnesses of the elements (Mulligan & MacLeod, 1988), and that in certain regimes observers could not distinguish luminance modulation from density modulation at threshold. In this paper we look in more detail at the luminance modulation thresholds for arrays of visually discrete elements, and compare the findings with existing models of contrast threshold and masking.

PROCEDURE

Stimuli consisted of one-dimensional sinusoidal luminance gratings. The gratings could be presented in two distinct modes: continuous (the usual stimuli for measuring contrast sensitivity) and sampled. The sampled case may be likened

*Present address: NASA/Ames Research Center, Mail Stop 239-3, Moffet Field, CA 94035, U.S.A.

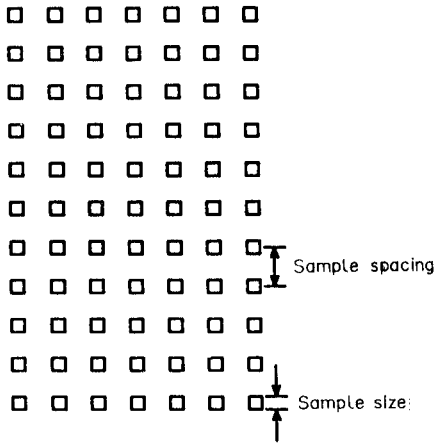


Fig. 1. Diagram of a portion of a sampling array defining the terms *sample spacing* (center-to-center distance between nearest neighbors) and *sample size* (linear height and width of a single square element).

to viewing a continuous grating through an opaque screen perforated with a regular array of small apertures. Thus sampling has the effect of reducing the overall space-average luminance (by a factor corresponding to the fraction of the total area occupied by the samples) and of restricting the information concerning the stimulus grating to the samples. The experiments described here used a sample array which consisted of small squares located on a regular two-dimensional grid.

Continuous gratings are characterized by their spatial frequency, orientation, and contrast. Sampled gratings require additional parameters to describe the nature of the sampling array: the sample size and shape, and the sample spacing. The meaning of these terms is illustrated in Fig. 1; sample spacing refers to the center-to-center distance between nearest neighbors in the lattice, while the sample size is the linear dimension of a single square element. It is sometimes convenient to talk about the *sample frequency*, which is just the reciprocal of the sample spacing. The sample frequency should be at least twice the grating or modulation frequency, in order to avoid spatial aliasing, which would cause the grating to appear at a much lower frequency. A sampling frequency of exactly twice the modulation frequency is generally known as the *Nyquist rate* (Oppenheim & Schaffer, 1975). When sampling at the Nyquist rate, the relative phase of the modulation and sample pattern becomes important: if the samples fall at the zero-crossings of the grating, no modulation will be transmitted. The stimuli in these experiments were always sampled at the peak and trough of the modulation waveform (in the Nyquist limit), and also at other points in the case of higher sample frequencies.

The *duty cycle* of a sample array will be defined to be the ratio of the sample size to the

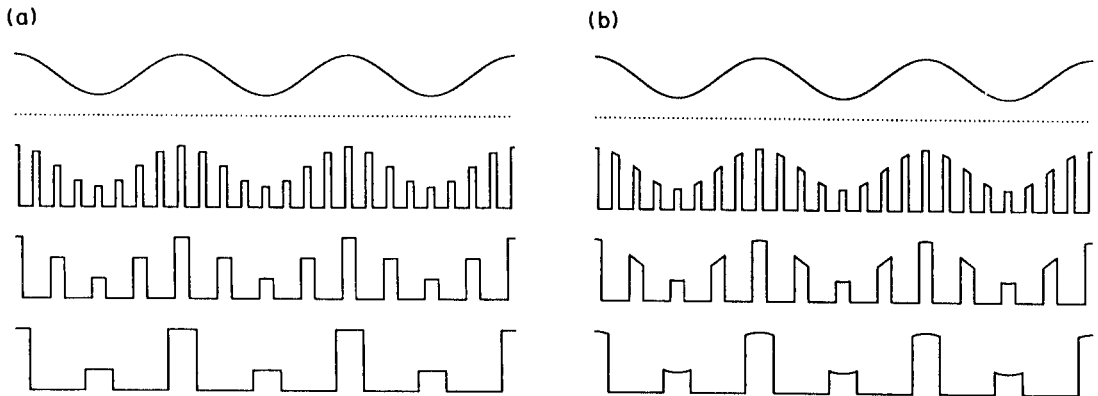


Fig. 2. (a) Intensity profiles for sampled gratings having the same modulation frequency, but different sample frequencies. At top is shown a continuous sinusoidal grating; the dotted line indicates the zero luminance baseline. Since the lowest point (trough) of the curve is halfway between the mean level and the baseline, this grating has a modulation of 50%. Immediately below is shown a sampled grating having the same modulation frequency and modulation depth, but sampled with eight samples per cycle. Also shown are four cycles per sample and two cycles per sample (the Nyquist limit). Note that each sample has a constant level (intensity) at each point within its interior. Also note that the sample width is proportional to sample spacing (constant duty cycle). These examples depict the duty cycle of 0.33 used in the experiments. (b) Same as in (a), but the samples depicted here are not uniform, but vary within their interiors in accordance with the corresponding patch of continuous gratings. This stimulus was not used in the experiments in this chapter, but is presented here to clarify the difference between the actual stimulus and the colloquial description: this is the stimulus which actually corresponds to viewing a grating through holes.

center-to-center sample spacing. In the experiments to be described, the duty cycle was kept fixed at one-third. Although this procedure confounded sample size and sample spacing, it allowed both the local sample luminance *and* the space-average luminance to be held constant at all sample spacings. The procedure thus allowed the separation of the spatial effects of the sampling operation from local effects dependent upon absolute luminance.

One important way in which the sampled stimulus differed from the analogy of viewing a grating through holes was that each sample was spatially uniform. The luminance for each sample was the same as the luminance of the continuous grating at the location of the center of the sample. This characteristic of the display produced a significant deviation from the continuous grating profile only for the larger sample sizes. Figure 2a shows the typical intensity profiles of rows of modulated samples for a variety of sample spacings. To illustrate the difference between the case of uniform samples (as used in these experiments, and shown in Fig. 2a) and a grating windowed, or viewed through holes, the latter case is also shown in Fig. 2b.

Stimuli were produced on a color monitor (Tektronix model 690SR), which received video signals from a graphics terminal (Advanced Electronic Devices model 767), which was in turn controlled by computer (Digital Equipment Corp. PDP 11/23). The display was viewed at a distance of 3 m, from which distance it subtended 4 deg of visual angle. Digital quantization errors in the rendering of the luminance profile were limited by the video digital-to-analog converter resolution (8 bits per phosphor). In order to decrease these errors, the display was viewed through a red filter (Kodak Wrattenno. 26), which had the effect of selectively attenuating the light from the green phosphor. The smallest test modulations could therefore be produced by varying the output of the green phosphor, with a high contrast background modulation provided by light from the red phosphor. This technique for reducing quantization errors has been discussed by Mulligan (1986).

The continuous gratings and samples had a mean luminance of 20 cd/m². The area surrounding the sample dots was dark. To see whether observed differences between the sampled and continuous cases were due to the overall luminance difference, the continuous sensitivities were remeasured using a one-log unit neutral density filter to reduce their space-average luminance

to a level comparable to that of the sampled gratings.

Thresholds were determined by having subjects discriminate between vertical and horizontal modulations. The orientation of the modulation was chosen at random for each trial. On each trial, the subject was presented with a grating whose orientation was selected at random; the subject's task was to correctly report the actual orientation. Each stimulus was visible for one second; the onset of the stimulus was preceded by a fixation cross which appeared in the middle of the (dark) screen one second before the stimulus appeared, and remained visible during the test interval. The $\frac{1}{2}$ deg square region containing the fixation target was kept free of sample dots. Modulation levels for successive trials were determined in accordance with a staircase procedure. The contrast was reduced after two consecutive correct responses, and increased after a single incorrect response, concentrating the trials near the contrast yielding 71% correct. Two staircases were randomly interleaved for each condition to minimize the amount of *a priori* information available to the subjects about the presentation on any given trial. A normal ogive anchored to 50% at zero contrast was fit to the observed probabilities using a weighted least squares regression, the complete details of which are given in Mulligan and MacLeod (1988). The weights were chosen to correct for the fact that the numbers of trials were not the same at each contrast, as well as the fact that the expected variability in the observations depended on the true underlying probability. Since these probabilities could not be known, we adopted an iterative procedure, wherein the observed probabilities were used to calculate the weights for the first iteration. The resulting psychometric function was then used to generate the weights for the second iteration. This was repeated until the estimates converged. Thresholds were taken to be the contrast for which the final fitted curve assumed a value of 75%.

Different modulation frequencies and sample spacings were run in different blocks of trials. The blocks for the different conditions were randomly interleaved, and each subject ran at least three blocks for every condition.

RESULTS

Typical data showing sensitivity for two different modulation frequencies as a function

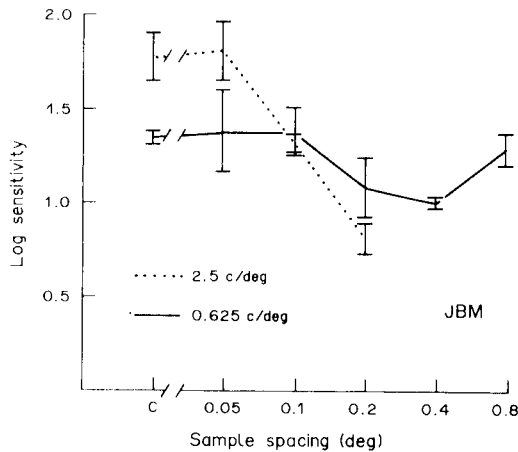


Fig. 3. Log sensitivity (reciprocal of threshold contrast) is shown as a function of sample spacing for subject JBM. Data points connected by solid lines are for a modulation frequency of 0.625 c/deg; dotted lines connect data points for 2.5 c/deg. The point on the abscissa labeled 'C' is for continuous gratings having a mean luminance equal to the mean sample luminance of the sampled gratings. Reduction of the mean luminance of the continuous stimuli to equal the space-average mean luminance of the sampled gratings produces only small changes in the continuous sensitivities (see text). Sensitivity is based on amplitude of sampled waveform (which differs from the amplitude of the Fourier component at the modulation frequency when sampling at the Nyquist rate). Error bars represent ± 2 SEM, computed between sessions.

of sample spacing is shown in Fig. 3. The point labeled "C" shows the sensitivity for modulation of a continuous field. The data show that sensitivity is unchanged, relative to continuous, for the smallest sample spacing; coarser sampling produces progressive losses of sensitivity. It is important to note that at the smallest sample spacing (3 min arc) the sample elements are still seen distinctly; thus the effects seen at coarser spacings cannot be due to changes introduced by sampling *per se*, such as the reduction in mean luminance or the introduction of black regions. For both frequencies shown, a sample spacing of 12 min arc is sufficient to produce the maximum sensitivity loss.

Sensitivity, as plotted in Fig. 3, is defined as the reciprocal of the threshold contrast. For the sampled gratings, the contrast was defined as the peak-to-trough amplitude divided by the mean sample luminance. Defined this way, a sampled grating always has the same contrast as the continuous grating behind the "holes". A discrepancy arises, however, if we redefine contrast based on the amplitude of the Fourier component at the modulation frequency. Figure 4 shows a plot of the amplitude of the

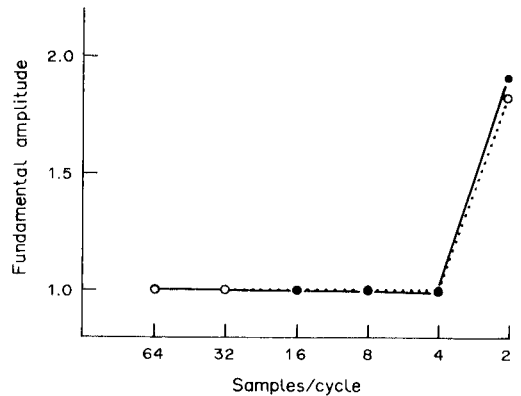


Fig. 4. Amplitude of the Fourier component at the fundamental modulation frequency as a function of the number of samples per cycle. Amplitudes are normalized relative to a continuous grating having the same mean luminance and contrast. The graph shows that sampling only affects the amplitude of the Fourier fundamental when sampling at two cycles per sample, where the amplitude of the fundamental roughly doubles. The solid curve is for uniform samples (as in Fig. 2a, the stimuli for these experiments), while the dotted lines link points for a windowed grating (as in Fig. 2b).

Fourier fundamental as a function of sample frequency. We see that this is almost independent of sample frequency except at the Nyquist limit, where it has approximately doubled. This is due to the fact that for Nyquist rate sampling, the aliases introduced by sampling have the same frequency as the signal, and can interfere either constructively or destructively depending on the relative phases of the sampling array and the modulation. The signal is maximized when the

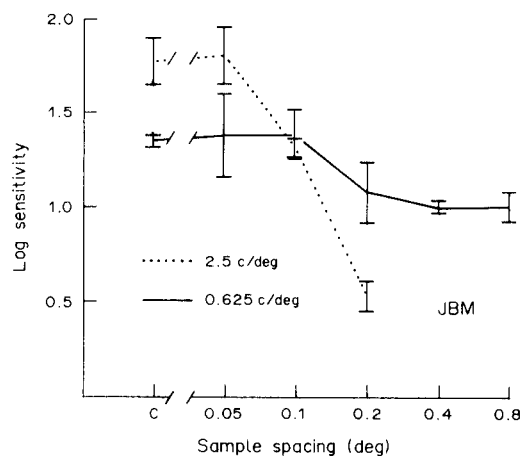


Fig. 5. The data from Fig. 3 are replotted with sensitivity redefined in terms of the amplitude of the Fourier component at the fundamental modulation frequency. Only the rightmost points of each curve are affected. This correction eliminates the nonmonotonicity seen in Fig. 3 for the 0.625 c/deg curve.

samples are placed at the peak and the trough (as in our stimulus). Note that if the samples are placed at the zero crossings of the grating, then there is complete destructive interference.

If we redefine sensitivity based on the reciprocal of the amplitude of the Fourier fundamental, the data shown in Fig. 3 would appear as shown in Fig. 5. Plotting the data this way eliminates the nonmonotonicity seen with the 0.625 c/deg grating at sample spacings greater than 0.2 deg.

Figure 6a shows sensitivity for sampled modulation (at 12 min sample spacing) and for continuous sinusoidal gratings plotted against modulation frequency. The data show that the sensitivity loss caused by sampling increases with increasing spatial frequency, becoming almost 1 log unit at 2.5 c/deg. The sensitivities for the sampled case were calculated on the basis of peak-to-peak amplitude, as in Fig. 3. The data may be replotted (Fig. 6b) using the sensitivity based on the amplitude of the Fourier funda-

mental; the only effect is to increase the sensitivity loss measured at 2.5 c/deg from 1.02 to 1.30 log units.

Reducing the mean luminance of the continuous gratings by a factor of 10 (with an optical filter) caused only a small loss of sensitivity for the spatial frequencies of interest, consistent with the results of Van Nes and Bouman (1967) for the range of mean luminances tested. For subject JBM, sensitivity was reduced by 0.23 log units (SEM = 0.021, between sessions) at a spatial frequency of 2.5 c/deg, and 0.046 log units (SEM = 0.015) at 0.625 c/deg.

Data for two additional subjects is shown in Fig. 7. These data were collected using a slightly different methodology, which is described in complete detail elsewhere (Mulligan, in preparation). A different technique was used to control quantization errors, which did not require the use of a red filter. This allowed a higher luminance to be used: the samples had a mean luminance of 120 cd/m²; the continuous gratings were viewed through a one-log unit neutral density filter to equate space-average mean luminances. Subjects used the method of adjustment to set thresholds. Six settings per point were made during each session, which were randomly interleaved with a number of additional conditions which are not discussed here. Each subject completed three sessions; a mean was computed for each session. The mean across sessions is plotted in Fig. 7, with the error bars showing ± 2 SEM computed between sessions.

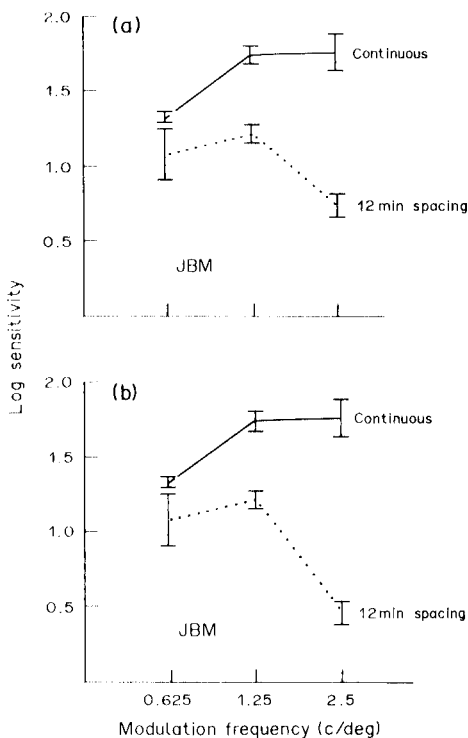


Fig. 6. (a) Log sensitivity for a single observer is plotted as a function of modulation frequency for continuous gratings (solid lines) and gratings sampled with a sample spacing of 12 min (dotted lines). Sensitivity is lower for the sampled gratings, and the loss increases with increasing modulation frequency. Error bars represent ± 2 SEM, computed between sessions. (b) The same data as in (a) is plotted with sensitivity defined in terms of the amplitude of the Fourier component at the fundamental modulation frequency. Only the rightmost point on the sampled curve is affected.

DISCUSSION

Elevation of threshold with coarse sampling

One of the major findings of this study is the elevation of contrast thresholds seen with increasing sample spacing. This result is not predictable on the basis of the physical limits on the information content in the stimulus; it can be shown that if detection were limited by photon noise statistics, we would expect to observe a constant threshold for the amplitude of the Fourier fundamental in the sampled stimulus regardless of the sample spacing (see Appendix). To explain the result, we can appeal to a mechanism suggested by data on increment threshold for a small test flash as a function of size of the background field (Westheimer, 1967; Buss, Hayhoe & Stromeyer, 1982). Increment threshold data are often displayed using a threshold vs intensity (*twi*) curve, where the flash

threshold is plotted as a function of the intensity of the background field. For large backgrounds, the curve has an asymptotic slope close to 1 on a log-log plot, showing that the threshold increment is proportional to the background level, a "Weber's law" relationship. This type of relation may be interpreted in terms either of a gain-control mechanism or of an approximately logarithmic nonlinearity, followed by a source of constant noise, with the threshold being met by exceeding a critical signal-to-noise ratio.

When such an experiment is done against a tiny (say, 5–10 min arc in diameter) adapting background, however, quite a different result is observed. The tiny background has a much greater desensitizing effect than a larger background having the same luminance, even though fewer total quanta strike the retina. Not only is the smaller background more effective, but at some (moderate) luminance level the threshold against the tiny background becomes infinite; the background seems to "saturate" the unit responsible for detection of the test. Results like this have been taken to be psychophysical consequences of the spatially opponent organization physiologically observed in retinal ganglion cells; a centrally excitatory zone ringed by an inhibitory annulus produces a unit whose response is relatively invariant under changes in absolute illumination level for spatially uniform stimulation.

Similar considerations of spatial opponency in early visual processing can help to explain the loss of sensitivity for coarsely sampled modulation. When the sample spacing is small, a spatially opponent unit will have some samples falling on its excitatory center, and others falling on its inhibitory surround. This results in a balanced state of excitation with adequate dynamic range to signal small changes in the amount of excitation or inhibition. Sample spacings which are large in relation to the dimensions of the receptive field will produce a state of affairs where most units will have only a single sample falling on their receptive field. If this sample falls entirely in an excitatory or inhibitory zone, the unit will be driven to an extreme of its response range, where it has poor differential sensitivity. If, on the other hand, the sample falls on the border between the excitatory and inhibitory zones, the unit's response will be maintained in the middle of its operating range; small modulations of the sample's luminance, however, will now not modulate the unit's output, since the modulations are seen both by the center and the

surround, with cancelling effects. In either case, the sampling operation should lead to reduced sensitivity.

Thus we see that center-surround antagonism can qualitatively account for some of the results we have observed, if we assume that the small concentric units responsible for the Westheimer effect are involved in the detection. This idea can be tested more rigorously by estimating the receptive field dimensions implied by our results, and comparing them to estimates obtained using other experimental paradigms. Westheimer's results (1967) suggest a surround diameter of 10 min arc in the central fovea. Ransom-Hogg and Spillmann (1980) performed similar experiments at various eccentricities; their data obtained at 5 deg temporal eccentricity suggests a surround diameter of about 1 deg. Since our experiments were performed using a centrally-fixated 4-deg field, we expect that the relevant receptive field size should have an intermediate value, in the range of 20–30 min. Our results (see Fig. 5) show no impairment of sensitivity at a sample spacing of 3 min arc, with progressive degradation up to 12 min. Assuming that maximal desensitization cannot occur until flanking dots are clear of the surround, the results shown in Fig. 5 suggest an upper bound on the surround radius of 0.2 deg, in good agreement with the results obtained from Westheimer's paradigm.

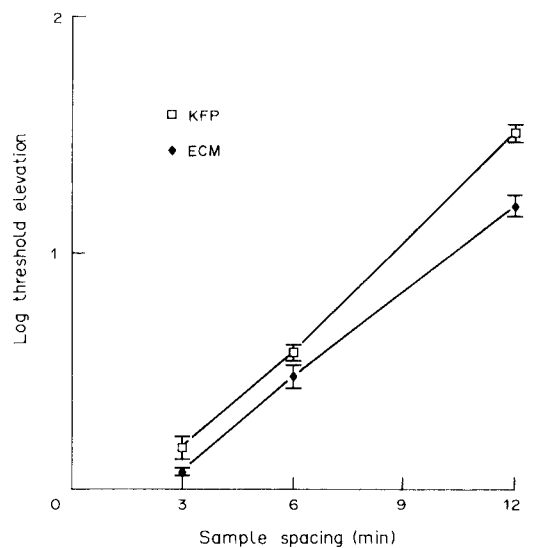


Fig. 7. Log threshold elevation as a function of sample spacing is shown for two additional subjects. The modulation frequency was 2.5 c/deg. Thresholds were obtained using method of adjustment, each subject completed three sessions, each consisting of six settings per point. The error bars represent ± 2 SE of the between sessions mean.

The data from the other subjects, shown in Fig. 7, suggest the same surround size to the extent that this crude estimate permits.

Burr, Ross and Morrone (1985) have reported sensitivity losses when a sinusoidal grating is discretely sampled by concentrating the light flux from the grating into thin lines parallel to the bars of the grating. They explained their results in terms of a local gain-control mechanism. One potential problem with their study, avoided in the present experiments, was the confounding of sample spacing with sample luminance. Since the results described here show strong effects of sample spacing even when local luminance is constant, the conclusions of Burr et al. concerning their own data must be reconsidered. Burr et al. plotted their results as a function of samples per cycle of modulation, which, because of their procedure, was inversely proportional to sample luminance. This obscures the effects of absolute sample spacing. However, when curves are drawn through their data linking points having the same absolute sample spacing, their results are similar to those shown in Fig. 6. Local gain-control may play a role in determining modulation sensitivity for sampled displays, but any mechanism that does not have a spatial component cannot produce a dependence of sensitivity on sample spacing or on modulation frequency; effects of both parameters are seen in the present study.

We have relied upon saturation of a spatially opponent unit to explain the elevation of threshold due to sampling. Another possible explanation, however, is that the frequency components introduced by the sampling lattice act as a mask and thereby elevate the threshold. Many effects of this type have previously been observed: measurements of the critical band suggest a channel bandwidth of one or two octaves (Stromeyer & Julesz, 1972; Henning, Hertz & Hinton, 1981). Although this could account for the increase in threshold for the highest modulation frequency, the sampling frequency is well outside of the critical band for the lower modulation frequencies. The masking model of Wilson, McFarlane and Phillips (1983) similarly predicts little masking of a 2 c/deg test by a 10 c/deg mask, whereas we observe a 0.5 log unit loss of sensitivity for a sampled 2.5 c/deg grating with a 6-min sample spacing (10 samples/deg). Thus we are forced to conclude that this type of masking alone cannot account for all of our data. One feature of the model of Wilson et al. is a parallel bank of spatial filters,

tuned to different spatial frequency bands. We propose that this split into spatial channels is preceded by a concentric spatially opponent layer (perhaps in the retina) which is responsible for the threshold elevations which we see which cannot be explained by critical band masking. It is interesting to note that Henning et al. (1981) proposed a similar two-stage model to account for masking by amplitude-modulated gratings.

Another piece of evidence consistent with the saturation hypothesis comes from similar experiments of Mulligan and MacLeod (1988), where a modulation could either be applied to the samples (as in the present experiments) or to the background (which, unlike the present experiments, had some small nonzero luminance). Under conditions which caused the largest sensitivity reductions (coarse sampling, high modulation frequency), the threshold elevations were from 2 to 4 times greater when the modulation was applied to the samples than when it was applied to the background. Since the modulations were at threshold, the mask was approximately the same in either case, and the results cannot therefore be explained in terms of simple masking. The fact that observers are less sensitive to modulation of the samples is consistent with saturation of the units conveying the samples' luminances, while the units responding to the background remain relatively sensitive.

Dependence of threshold elevation upon modulation frequency

Although saturation of spatially opponent neurons can explain the observed relation between threshold elevation and sample spacing, it does not predict the dependence of the elevation on modulation frequency shown in Fig. 6. One explanation for the dependence of threshold elevation on modulation frequency is that the masking effect seen at low modulation frequencies (which we have assumed to be due to a saturating spatially opponent unit) is augmented at higher modulation frequencies by traditional critical band masking of the modulation signal by the spatial frequency components introduced by the sampling operation. The fundamental component of these added frequencies has a period equal to the sample spacing; this is always higher than the modulation frequency, but is closest for the highest modulation frequency. Because the masking effects normally increase with proximity in frequency, the present

observed dependence on modulation frequency is to be expected, at least qualitatively.

We can make a slightly more quantitative prediction using the model predictions of Wilson et al. (1983). Their model predicts a sensitivity loss of approximately a factor of 4 for a 2 c/deg test on a 4 c/deg oblique mask of 40% contrast. This mask is not probably somewhat weaker than that used in our experiments, where the sampling array had components at the *same* orientation of the test, the effective contrast of which was closer to 50%. Therefore it might be reasonable to assume that critical band masking is responsible for most of the 0.75 log units of additional threshold elevation that is seen on under coarsely sampled conditions when the modulation frequency is raised from 1.25 to 2.5 c/deg (Fig. 6b).

Some evidence that sensitivity losses due to sampling are *not* simple masking effects comes from the previously mentioned study done by Burr et al. (1985). Using a slightly different stimulus, they also observed sensitivity losses in the presence of sampling. To rule out the possibility of masking, they created a second stimulus having the same power spectrum as the original, but with scrambled phase relationships between individual frequency components. The large threshold elevations vanished under these conditions. It might be argued that a scrambled phase masker *should* have a weaker effect than a particularly chosen mask of the same power spectrum, since the scrambled phase mask will have its energy distributed over most of the units making up the tuned channel, while the signal information will be carried by a subset of the units whose phase sensitivity matches the signal. In this case, however, we would still expect to see some residual masking effect of the scrambled-phase masker, since *some* of the mask energy would still be carried by the units carrying the signal information. The data of Burr et al., however, show that there is little threshold elevation due to the scrambled phase mask; what effects remain are identical even when the one-dimensional mask is rotated 90 deg. Additional results demonstrating the phase sensitivity of masking have been demonstrated by Henning, Hertz and Broadbent (1975), but the effects are smaller than those observed by Burr et al. Similar differences in masking efficacy between masks which are either correlated or uncorrelated with the target pattern have been demonstrated by Rentschler, Hubner, Caelli and Stoerig (1986).

General discussion

We have seen that the results presented in this paper cannot be accommodated by a single tuned filter which mediates detection, although critical band masking may be part of the explanation for the dependence of threshold elevation upon modulation frequency. Similar conclusions have been reached by Henning et al. (1975). Henning et al. investigated the interactions between an amplitude modulated grating having a moderately high carrier frequency and a low-frequency grating at the modulation frequency. (The amplitude modulated stimulus is in some ways analogous to what we have called a "sampled grating"; the Fourier components in the sampling lattice function as the carrier.) They observed substantial masking effects between frequency bands that appear to be independent when probed with noise masks such as those used by Stromeyer and Julesz (1972) and Henning et al. (1981). One model proposed by Henning et al. (1975) to explain their results consisted of two stages, where units in the second stage having large, spatially opponent receptive fields received both a direct input and an input from units in the first stage having small, spatially opponent receptive fields. Thus, the second-stage units responded both to low-frequency modulation and to contrast modulation of a high-frequency pattern capable of exciting the first-stage units.

Spatial frequency analysis was also rejected by Nyman and Laurinen (1982) to explain their results concerning the perception of sparsely sampled waveforms. They investigated discrimination of sampled square and sine waves, and found that performance was *better* than would have been expected on the basis of the detectability of the extra frequencies present in the square-wave stimulus. They attributed their findings to local feature analyzers. One point they mention in passing, but do not discuss, is that the discrimination becomes easier if the viewing distance is increased. Increasing the viewing distance increases both the grating frequency and sampling frequencies proportionately. This observation is interesting in light of the results presented in this paper, where we have seen that increasing sample frequency improves the visibility of sampled gratings.

In tuned filter models of modulation sensitivity the stimulus is assumed to be detected when some individual detector in the array reaches

a threshold signal level. Another possibility, particularly plausible for the sampled case, is that detection is mediated by a spatial *comparison* of the outputs of filters at different locations. Detection of the sampled grating might be mediated by a spatial comparison of the brightnesses of various elements in the sample lattice (based on signals representing the local contrast or luminance of individual elements). If we assume that threshold in the continuous case is *not* mediated by the same type of brightness discrimination mechanism, then the difference in the spatial frequency dependence of the threshold in the sampled case may be explained by assuming that signals contributing to brightness undergo different spatial processing. Experiments involving density modulation of dot arrays have indicated that changes in local dot density are sometimes perceived as changes in dot brightness (Mulligan & MacLeod, 1988). The results of these studies indicate a large summation area for brightness, roughly 1 deg in diameter. Such a mechanism would be expected to increase threshold for sampled modulation at high modulation frequencies assuming that a brightness discrimination is involved in detecting the sampled modulation but *not* in the detection of continuous gratings. This assumption seems reasonable since an edge-detecting mechanism with good spatial resolution which saturates at moderate contrast levels would not see any difference in the sample arrays when the modulation is applied, but could easily signal the presence of light and dark grating bars in a continuous field.

In conclusion, sampling has been seen to degrade contrast sensitivity when the sample spacing is greater than or equal to 12 min arc. The largest effects are seen with higher modulation frequencies, where they can be as large as one log unit. Response saturation of spatially opponent units can explain the dependence of the threshold elevation on sample spacing, and the results of this study are in good quantitative agreement with the results of previous studies. The dependence upon modulation frequency, however, cannot be explained by this mechanism, but might be explained by an additional critical band masking effect.

Acknowledgements—This work was supported by NIH grant EY-01711 and an IBM graduate fellowship awarded to JBM. Additional support for the work has been received from NASA RTOP 505-67.

REFERENCES

- Burr, D. C., Ross, J. & Morrone, M. C. (1985). Local regulation of luminance gain. *Vision Research*, *25*, 717–727.
- Buss, C. M., Hayhoe, M. M. & Stromeyer, C. F. III (1982). Lateral interactions in the control of visual sensitivity. *Vision Research*, *22*, 693–709.
- Campbell, F. W. & Robson, J. G. (1968). Application of Fourier analysis to the visibility of gratings. *Journal of Physiology, London*, *197*, 551–566.
- Cornsweet, T. N. (1970). *Visual perception*. New York: Academic Press.
- Georgeson, M. A. & Sullivan, G. D. (1975). Contrast constancy: Deblurring in human vision by spatial frequency channels. *Journal of Physiology, London*, *252*, 627–656.
- Green, D. M. & Swets, J. A. (1966). *Signal detection theory and psychophysics*. New York: Wiley.
- Henning, G. B., Hertz, B. G. & Hinton, J. L. (1981). Effects of different hypothetical detection mechanisms on the shape of spatial-frequency filters inferred from masking experiments—I. Noise masks. *Journal of the Optical Society of America*, *71*, 574–581.
- Henning, G. B., Hertz, B. G. & Broadbent, D. E. (1975). Some experiments bearing on the hypothesis that the visual system analyses spatial patterns in independent bands of spatial frequency. *Vision Research*, *15*, 887–897.
- Land, E. H. & McCann, J. J. (1971). Lightness and the retinex theory. *Journal of the Optical Society of America*, *61*, 1–11.
- Mulligan, J. B. (1986). Optimizing stereo separation in color television anaglyphs. *Perception*, *15*, 27–36.
- Mulligan, J. B. & MacLeod, D. I. A. (1988). Reciprocity between luminance and dot density in the perception of brightness. *Vision Research*, *28*, 503–519.
- Nyman, G. & Laurinen, P. (1982). Reconstruction of spatial information in the human visual system. *Nature, London*, *297*, 324–325.
- Olzak, L. A. & Thomas, J. P. (1986). Seeing spatial patterns. In Boff, K. R., Kaufman, L. & Thomas, J. P. (Eds.), *Handbook of perception and human performance* (pp. 7-1–7-56). New York: Wiley.
- Oppenheim, A. V. & Schaffer, R. W. (1975). *Digital signal processing*. Englewood Cliffs, NJ: Prentice-Hall.
- Ransom-Hogg, A. & Spillmann, L. (1980). Perceptive field size in fovea and periphery of the light- and dark-adapted retina. *Vision Research*, *20*, 221–228.
- Rentschler, I., Hubner, M., Caelli, T. & Stoerig, P. (1986). Structural masking revealed by extrafoveal image recognition. *Investigative Ophthalmology and Visual Science (Suppl.)*, *27*, 95.
- Stromeyer, C. F. III & Julesz, B. (1972). Spatial-frequency masking in vision: Critical bands and the spread of masking. *Journal of the Optical Society of America*, *62*, 1221–1232.
- Van Nes, F. L. & Bouman, M. A. (1967). Spatial modulation transfer in the human eye. *Journal of the Optical Society of America*, *57*, 401–406.
- Westheimer, G. (1967). Spatial interaction in human cone vision. *Journal of Physiology, London*, *190*, 139–154.
- Wilson, H. R. & Bergen, J. R. (1979). A four mechanism model for threshold spatial vision. *Vision Research*, *19*, 19–32.
- Wilson, H. R., McFarlane, D. K. & Phillips, G. C. (1983). Spatial frequency tuning of orientation selective units estimated by oblique masking. *Vision Research*, *23*, 873–882.

APPENDIX

A Proof that Detectability is Unaffected by Sampling Rate for an Ideal Observer

Definition of terms

- T = Total number of quanta in one grating cycle.
- N = Number of samples per grating cycle.
- n_i = Mean number of quanta in the i th sample when signal not present ($n_i = T/N$).
- A = Amplitude of sampled modulation as a fraction of the mean (relative amplitude).
- s_i = Expected or ensemble average signed increment in the number of quanta at i th sample due to signal modulation when present [$s_i = An_i \cos(2\pi i/N)$].
- e_{it} = Noise at i th sample on the t th presentation, deviation from expected number of quanta.
- σ_e = Expected r.m.s. value of e_{it} [$\sigma_e = \sqrt{n_i}$, by assumptions (1) and (2) below].
- o_{it} = Number of quanta observed at i th sample on the t th presentation ($o_{it} = n_i + s_i + e_{it}$ when signal present, $o_{it} = n_i + e_{it}$ otherwise).

Our analysis is patterned after the approach of Green and Swets (1966) to the ideal detector for the case when the signal is known exactly. The proof depends on the following assumptions: (1) that the mean number of quanta per sample n_i is large enough that we may approximate the noise due to Poisson variability as a random variable having a Gaussian distribution about a mean of zero with a variance of n_i (for the conditions of the experiments, assuming a 3 mm natural pupil, the total number of quanta absorbed during a single stimulus presentation is on the order of 6 million); (2) that the noise at a given sample e_{it} is independent of i (and therefore uncorrelated with the signal s_i and with the noise at any other sample e_{it}); (3) that $s_i \ll n_i$ for the near-threshold conditions of interest; this assumption allows us to neglect the effect of the signal on σ_e . With these assumptions, we can show that the detectability of the signal does not depend on N , the number of samples, for values of N divisible by 4 (that is, for all the conditions of the experiments except the Nyquist case).

An ideal observer will report the presence of the signal if the *likelihood ratio* is greater than one. The likelihood ratio is the ratio of two conditional probabilities: the probability of making the observation in the presence of the signal and the probability of making the same observation in the absence of the signal.

To find the probability of making a particular set of observations $\{o_{it}\}$ in the case of a particular signal $\{s_i\}$, we assume that the signal was present, and therefore any deviations between the observed values and the signal must be due to quantum fluctuations ($o_{it} = n_i + s_i + e_{it}$). The probability of making the observation $\{o_{it}\}$ in the presence of the signal is just the probability of quantum fluctuations producing the set of deviations $\{e_{it}\}$.

Because we have assumed that the noise e_{it} has a Gaussian distribution, we can write the probability of a particular value for e_{it} as:

$$P(e_{it}) = \frac{1}{\sqrt{2\pi\sigma_e}} \exp\left(-\frac{e_{it}^2}{2\sigma_e^2}\right). \quad (\text{A1})$$

The probability for a given N -tuple $\{e_{it}\}$ is simply the product of N such terms. We can transform this product to a sum by taking the natural logarithm; the log of the

probability of making the observation $\{o_{it}\}$ in the presence of the signal, which we shall refer to as L_s , is therefore:

$$L_s = K_0 - K_1 \sum_{i=1}^N [o_{it} - (n_i + s_i)]^2; \quad (\text{A2})$$

where

$$K_0 = N \ln\left(\frac{1}{\sqrt{2\pi\sigma_e}}\right), \quad \text{and} \quad K_1 = \frac{1}{2\sigma_e^2}.$$

We can similarly express the log of the probability that the same set of observations $\{o_{it}\}$ would be made in the absence of the signal:

$$L_0 = K_0 - K_1 \sum_{i=1}^N (o_{it} - n_i)^2. \quad (\text{A3})$$

Now the ideal observer bases his decision on the ratio of the conditional probabilities, which is equivalent to taking the difference of the logs of the probabilities; therefore, the ideal observer will report seeing the signal if $(L_s - L_0) > 0$. The proof will consist in showing that the sign of this difference does not depend on N :

$$L_s - L_0 = -K_1 \left[\sum_{i=1}^N (o_{it} - n_i - s_i)^2 - \sum_{i=1}^N (o_{it} - n_i)^2 \right].$$

By expanding the squared quantities and cancelling terms (taking out the leading minus sign in the process), this may be expressed as

$$L_s - L_0 = K_1 \left[2 \sum_{i=1}^N s_i (o_{it} - n_i) - \sum_{i=1}^N s_i^2 \right]. \quad (\text{A4})$$

The second sum depends only on the signal; the first sum represents the correlation between the observed numbers of quanta and those expected if there is a signal. Let us first consider the value of the second sum. For cosine phase sinusoidal modulation $s_i = An_i \cos(2\pi i/N)$. By the symmetry of the sine function, $s_i = -s_{i+N/2}$; therefore,

$$\sum_{i=1}^N s_i^2 = 2A^2 n_i^2 \sum_{i=1}^{N/2} \cos^2\left(\frac{2\pi i}{N}\right). \quad (\text{A5})$$

Since we have assumed that N is divisible by four, we may break this sum into two halves:

$$\begin{aligned} \sum_{i=1}^N s_i^2 &= 2A^2 n_i^2 \left[\sum_{i=1}^{N/4} \cos^2\left(\frac{2\pi i}{N}\right) + \sum_{i=1+N/4}^{N/2} \cos^2\left(\frac{2\pi i}{N}\right) \right], \\ &= 2A^2 n_i^2 \sum_{i=1}^{N/4} \left[\cos^2\left(\frac{2\pi i}{N}\right) + \cos^2\left(\frac{2\pi(i+N/4)}{N}\right) \right], \\ &= 2A^2 n_i^2 \sum_{i=1}^{N/4} \left[\cos^2\left(\frac{2\pi i}{N}\right) + \sin^2\left(\frac{2\pi i}{N}\right) \right], \\ &= 2A^2 n_i^2 N/4. \end{aligned}$$

Since $n_i = T/N$ by definition, we may simplify the result to:

$$\sum_{i=1}^N s_i^2 = \frac{A^2 T^2}{2N}. \quad (\text{A6})$$

In the case of modulation at the Nyquist frequency, the sum in equation (A5) has only a single term which has a value of 1 for the cosine phase modulation we are considering. In this case: $\sum_{i=1}^N s_i^2 = (A^2 T^2)/2$.

Now the first sum in equation (A4) is two times the covariance between the signal s_i and the deviations of the

observed values from the no-signal mean, $(o_{it} - n_i)$. Let us refer to this covariance as C_t . When no signal is present (so that $o_{it} = n_i + \epsilon_{it}$),

$$C_t = \sum_{i=1}^N s_i \epsilon_{it};$$

since we have assumed that the noise ϵ_{it} is independent of the signal, this quantity has an expected value of zero. When the signal is present (so that $o_{it} = n_i + s_i + \epsilon_{it}$,

$$C_t = \sum_{i=1}^N s_i \epsilon_{it} + \sum_{i=1}^N s_i^2;$$

in addition to the first term (which has an expected value of zero), there is a second constant term, which has a value of $A^2 T^2 / 2N$ from equation (A6). The variance C_t is the same whether or not the signal is present, and is just the variance of the term $\sum_{i=1}^N s_i \epsilon_{it}$. This variance in turn is just the sum of the variances of the individual terms $s_i \epsilon_{it}$. We may therefore write:

$$\begin{aligned} \sigma_c^2 &= \sum_{i=1}^N s_i^2 \sigma_c^2, \\ &= \sigma_c^2 \sum_{i=1}^N s_i^2, \\ &= n_i \frac{A^2 T^2}{2N}; \end{aligned}$$

using the definition of σ_c and the result of equation (A6). Remembering again that $n_i = T/N$, the result may be expressed as:

$$\sigma_c^2 = \frac{A^2 T^2}{2N^2}. \tag{A7}$$

Thus we see that:

$$L_s - L_0 = K_1 \left(2C_t - \frac{A^2 T^2}{2N} \right);$$

which has an expected value of $-K_1(A^2 T^2 / 2N)$ when no signal is present and expected value of $K_1(A^2 T^2 / 2N)$ in the presence of the signal. The variance of the quantity $(L_s - L_0)$ does not depend on the presence of the signal and is equal to $4K_1^2$ times σ_c^2 . Since the presence of the signal affects only the sign of the expected value of $(L_s - L_0)$, the signal-to-noise ratio does not depend on the presence of the signal and is:

$$SNR = \frac{K_1 0.5 A^2 T^2 N^{-1}}{2K_1 \sigma_c};$$

which by substitution of the value of σ_c from equation (A7) becomes

$$\begin{aligned} &= \frac{K_1 0.5 A^2 T^2 N^{-1}}{K_1 A T N^{-1} \sqrt{2T}} \\ &= \frac{A \sqrt{T}}{2\sqrt{2}}. \end{aligned}$$

Since this does not depend on N , the proof is complete.

The only part of our proof which depended on N being a multiple of 4 was the calculation of $\sum_{i=1}^N s_i^2$ which resulted in equation (A6). It was noted above that this quantity has a value of $A^2 T^2 / 2$ for the case of Nyquist sampling. Note that this a factor of 2 larger than what would be obtained by simply substituting $N = 2$ into equation (A6). Because this quantity is also the expected value of C_t , the log of the likelihood ratio, $(L_s - L_0)$, is proportional to it. In addition, the variance σ_c is proportional to $\sum_{i=1}^N s_i^2$. By recomputing the signal-to-noise ratio using these revised values, it is easy to show that it has a value $\sqrt{2}$ higher than for the non-Nyquist case.